Ontario Hydro

RESEARCH DIVISION

91602
new 82-10

COMPLIMENTARY COPY
Please Credit Ontario Hydro Research if
Reproduced in Whole or in Part.

ontario hydro
research division

TECHNICAL ASSISTANCE TO AECL ELECTRON BEAM WELDING OF THICK-WALLED COPPER CONTAINERS FOR NUCLEAR FUEL WASTE DISPOSAL - PHASE TWO

Report No 84-57-K

P.Y.Y. Maak
Engineer - Metallurgy Section
Metallurgical Research Department

ABSTRACT

This report describes the results of Phase Two of the copper electron beam welding project for the final closure of copper containers for nuclear fuel waste disposal. It has been demonstrated that single pass, electron beam square butt welds (depth of weld penetration >25 mm) can be made without preheat in both electrolytic tough-pitch copper and oxygen-free copper plates. The present results show that oxygen-free copper exhibits better weldability than the electrolytic tough-pitch copper in terms of weld penetration and vulnerability to weld defects such as gas porosity, erratic metal overflow and blow holes. The results of ultrasonic inspection studies of the welds are also discussed.

job	file	date	report no.
740681-144-461	823.241	May 28, 1984	84-57-K

91602
new 82-10

ontario hydro
research division

EXECUTIVE SUMMARY

ELECTRON BEAM WELDING OF THICK-WALLED COPPER CONTAINERS FOR NUCLEAR FUEL WASTE DISPOSAL - PHASE TWO

P.Y.Y. Maak

As part of Ontario Hydro's technical assistance to the Canadian Nuclear Fuel Waste Management Program, the Welding Research Unit of the Metallurgical Research Department is investigating the feasibility of using electron beam welding for the final closure of copper containers for nuclear fuel waste disposal. This investigation has been divided into three phases. The first and second phases have been completed. A general outline of the present project and the results of Phase One have been reported /1/.

This report describes the results of Phase Two. The present results show that square butt electron beam welds (depth of penetration > 25 mm) can be made without preheat in both electrolytic tough-pitch (ETP) copper and oxygen-free (OF) copper plates using more than one combination of weld parameters. It was shown that combinations of high beam power and high welding speed are preferred in electron beam welding of thick copper. The OF copper contained less dissolved oxygen in the base metal and, thus, exhibited much better weldability than the ETP copper. In comparison with the ETP copper welds, sound OF copper welds could be made using a much wider range of beam power and welding speed, without producing significant amounts of gas porosity in the fusion zone or erratic metal overflow and blow holes on the weld surface.

Results of ultrasonic inspection studies on welded samples indicated that relatively large cavities in the fusion zone are more readily detected than smaller cavities due to gas porosity. However, it was questionable whether lack of fusion where the joint was missed by the electron beam could be detected in the copper welds.

B.M.

job	file	date	report no.
740681-144-461	823.241	May 28, 1984	84-57-K

TABLE OF CONTENTS

		Page
1.0	INTRODUCTION	1
2.0	EXPERIMENTATION IN PHASE TWO	1
	2.1 Material	1
	2.2 Welding Trials	2
	2.3 Ultrasonic Inspection Studies	2
3.0	EXPERIMENTAL RESULTS	2
	3.1 Electrolytic Tough-Pitch Copper Welding Studies	2
	3.1.1 Combinations of Low Beam Power/ Low Welding Speed Parameters	2
	3.1.2 Combinations of High Beam Power/ High Welding Speed Parameters	3
	3.1.3 Focus Position	3
	3.1.4 Welding Current	4
	3.1.5 Accelerating Voltage	4
	3.2 Oxygen-Free Copper Welding Studies	4
	3.3 Ultrasonic Inspection of Copper Electron Beam Welds	5
	3.3.1 C-Scan Maps	5
	3.3.2 Welds in Test Numbers 3 and 16	5
	3.3.3 Welds in Test Numbers 6 and 19	6
	3.3.4 Welds in Test Numbers 7 and 20	6
4.0	DISCUSSION	7
	4.1 Weld Penetration and Weld Profile	7
	4.2 Porosity, Cavities and Metal Overflow	8
	4.2.1 Electrolytic Tough-Pitch Copper	8
	4.2.2 Oxygen-Free Copper	9
	4.3 Copper Oxide	9
	4.4 Missed Joint	10
	4.5 Ultrasonic Inspection	10
	4.6 Empirical Equation for the Penetration of Copper Electron Beam Welds	11

TABLE OF CONTENTS

		Page
5.0	WORK AREAS IN PHASE THREE	13
5.1	Phase 3A: Optimization of Welding Parameters	13
5.2	Phase 3B: Electron Beam Welding of Small-Scale Thick-walled Copper Pipe Mockups	13
6.0	CONCLUSIONS	14
ACKNOWLEDGEMENT		15
REFERENCES		16
TABLES		
FIGURES		
DISTRIBUTION		last page

LIST OF TABLES

		Page
TABLE I	Chemical Specification For Electrolytic Tough Pitch Copper (UNS No 110) and Oxygen-Free Copper (UNS No 101)	17
TABLE II	Details of Welding Trials in Phase Two	18
TABLE III	Weld Penetration and Weld Width	19
TABLE IV	Penetration Equation for Electron Beam Welding of Thick Copper	20

LIST OF FIGURES

Figure 1 Schematic Diagram Showing the Final Closure Joint Design with Integral Backing Support for a Copper Container for Nuclear Fuel Waste Disposal

Figure 2 Schematic Examples Showing the Set-up for Ultrasonic Inspection of Copper Electron Beam Welded Samples

Figure 3 Cross-sections of Electrolytic Tough-pitch Copper Welds (3.5X)

Figure 4 Typical Microstructure of Electrolytic Tough-pitch Copper Electron Beam Welds (600X)

Figure 5 Surface Appearance of Electrolytic Tough-pitch Copper Welds in Tests 1 to 7

Figure 6 Cross-sections and Surface Appearance of Electrolytic Tough-Pitch Copper Welds in Tests 8 to 9 (0.5X)

Figure 7 Cross-sections of Electrolytic Tough-pitch Copper Welds Made with Electron Beam Focussed at Various Positions Below the Surface (3.5X)

Figure 8 Cross-sections of Electrolytic Tough-pitch Copper Welds Made at Increasing Welding Current (3.5X)

Figure 9 Cross-sections of Electrolytic Tough-pitch Copper Welds Made at Increasing Voltage (3.5X)

Figure 10 Cross-sections of Oxygen-free Copper Welds in Tests 16, 17, 19 and 20 (3.5X)

Figure 11 Surface Appearance of Oxygen-free Copper Welds (0.5X)

Figure 12 Typical Microstructure of Oxygen-free Copper Electron Beam Welds (600X)

Figure 13 C-Scan Maps for Welds in Tests 3 and 16

Figure 14 C-Scan Maps for Welds in Tests 6 and 19

Figure 15 C-Scan Maps for Welds in Tests 9 and 20

Figure 16 Predicted Weld Penetration Versus Measured Weld Penetration

91601
new 82-10

ontario hydro
research division

To Mr. H.N. Issac
Manager
Nuclear Materials Management
Design and Development Division

ELECTRON BEAM WELDING OF THICK-WALLED COPPER CONTAINERS FOR NUCLEAR FUEL WASTE DISPOSAL - PHASE TWO

1.0 INTRODUCTION

As part of Ontario Hydro's technical assistance to the Canadian Nuclear Fuel Waste Management Program, the Welding Unit of the Metallurgical Research Department, Ontario Hydro, is developing an optimum electron beam (EB) welding procedure for the final closure of thick-walled (~25 mm thick) copper containers for nuclear fuel waste disposal.

In Phase One of this project, it was demonstrated that single pass, EB welds could be made without preheat in 50-mm-thick electrolytic tough-pitch (ETP) copper plates/1/. In addition, a preferred joint design with integral backing support was proposed /1/ (see Figure 1).

This report describes the results obtained in Phase Two. Single pass, square butt welds were made in 25-mm-thick ETP and OF copper plates using the EB welding process, and the effect of welding parameters on the weld quality was evaluated. Ultrasonic inspection was one of the techniques used to evaluate the welded samples.

2.0 EXPERIMENTATION OF PHASE TWO

2.1 Material

Electron beam welding trials were carried out on copper workpieces, 25 mm thick, ~113 mm long and 24 mm wide. Both ETP copper (UNS No. 110) and OF copper (UNS No 101) plates were used.

The chemical specifications for these two grades of copper are shown in Table I/2/. The OF copper is purer (99.99%) than the ETP copper and contains a maximum of 0.001% dissolved oxygen. ETP copper is 99.9% pure and contains 0.02 to 0.07% dissolved oxygen.

2.2 Welding Trials in Phase Two

The welding trials were performed at the National Research Council (NRC), Ottawa. The electron gun is rated at 42-kW beam power, with an accelerating voltage of 60 kV and a maximum beam current of 700 mA.

Square butt welds were made in 25-mm-thick ETP and OF copper plates with the use of backing plates. The details of the welding trials are given in Table II. The welding parameters investigated were beam current, accelerating voltage, welding speed and beam focus position. The welded samples were sent to Ontario Hydro for metallurgical evaluation.

2.3 Ultrasonic Inspection Studies

To investigate the inspectability of copper EB joints, welded samples from tests 3, 6, 9, 16, 19 and 20 were examined ultrasonically using

(1) A Branson driving system with a water tank.
(2) An Apple II microcomputer with a Blue Tank Program.
(3) A KB-6000 ultrasonic instrument.
(4) A "KB-Aerotech Gamma" 5.0 MHz/12.7 mm immersion probe and a "Harisonic" 15 MHz, 50 mm focus and 9.38 mm diameter probe.

The normal-beam, fusion-line, pulse-echo technique was used to scan the entire thickness of the samples using the set-up shown in Figure 2. C-scan maps, showing the location of various weld defects, were obtained.

3.0 EXPERIMENTAL RESULTS

3.1 Electrolytic Tough-Pitch Copper

3.1.1 Low Beam Power/Low Welding Speed Studies

In tests 1 to 7, welds were made using various combinations of beam power and welding speed with the heat input constant at ~26.6 kJ/cm (67.5 kJ/in). The depth of penetration and width of the welds are given in Table III, except for numbers 1 and 5. Welds made at relatively low welding speed and low beam power (welds 2 to 4) displayed weld penetrations of less than 25 mm. Welds, made at higher welding speed and beam power (welds 6 and 7) exhibited greater weld penetration (25 to 30 mm). The cross sections of these welds, shown in Figure 3, indicate that the total fused area increased with increasing beam power and welding speed, for a constant heat input.

Apparently, the power efficiency increased with increasing welding speed for the welding speeds tested, ie, 3.4 mm/s (8 in/min) to 8.5 mm/s (20 in/min).

Welds 1 to 7, the fusion zone tapered from a wide upper zone to a line joint at the underbead (see Figure 3). In welds 2 and 3, the underbeads narrowed to a "dagger edge", which appeared to miss the joint interface. Root cavities were detected in welds 3, 4 and 7.

Welds 1 to 7 all displayed porosity throughout the fusion zone, (see Figure 3). Also, as illustrated in Figure 4, discrete oxide particles were found in these welds, although no oxide film was found at the grain boundaries as has been previously observed/1/. All these welds displayed smooth metal overflow on the weld surface (see Figure 5).

3.1.2 High Beam Power/High Welding Speed Studies

High welding speeds of 25.4 mm/s (60 in/min) and 33.9 mm/s (80 in/min) and a high beam power level of 42 kW were used in tests 8 and 9, respectively (see Table II). Both welds displayed a parallel-sided fusion zone, as shown in Figure 6(a). With all other parameters held constant, weld 8, which was made at the slower welding speed, displayed greater weld penetration (32.3 mm) than weld 9 (27.7 mm).

These two welds contained less gas porosity than the welds made at relatively low welding speeds, ie, tests 1 to 7; however, large cavities were found in the fusion zone of welds 8 and 9 (see Figure 6(a)). The welds also exhibited erratic molten metal overflow and blow holes on the surface, which appeared to have resulted from violent gas-metal interaction during the welding process (see Figure 6(b)). Weld 9, which was made at higher weld speed, appeared to have suffered from more violent molten metal-metal vapour interaction than weld 8. Discrete oxide particles were detected in both these welds.

3.1.3 Electron Beam Focus Position

Welds 4, 10 and 11 were made at EB focus positions of 8.5 mm 16.9 mm and 25.4 mm below the surface of the copper workpieces respectively.

With other welding parameters held constant, the focus position did not appear to affect weld penetration (see Table III). At a focus position 8.5 mm below the surface, the fusion zone of weld 4 was more parallel-sided with a wider underbead than

welds 10 and 11, which were focussed at greater depths (see Figure 7). Welds 10 and 11 both displayed a wide upper bead and a "dagger edge" underbead.

Under the present welding conditions, the focus position did not affect the gas porosity in the fusion zone noticeably (see Figure 7).

3.1.4 Welding Current

With other welding parameters held constant, welds 12, 4 and 13 were made at welding currents of 325 mA, 350 mA and 375 mA, respectively. The weld penetration increased from 21.1 mm to 29.4 mm with an increase in current from 325 to 375 mA (see Table III). A higher welding current also appeared to promote the formation of a more parallel-sided fusion zone (see Figure 8). Within this range of welding current, an increase in current did not affect the level of gas porosity in the fusion zone noticeably.

3.1.5 Accelerating Voltage

With other parameters held constant, welds 14, 4 and 15 were made at voltage levels of 40, 45 and 50 kV, respectively. The depth of weld penetration increased from 18.9 mm in weld 14 to 25 mm in weld 15 as the voltage increased from 40 to 50 V (see Table III). As the voltage, and thus the beam power, increased, the weld shape became more parallel-sided (see Figure 9).

3.2 Oxygen-Free Copper

Welds 16 to 20 were made in 25-mm-thick OF copper using the same parameters as for welds 3, 4, 6, 8 and 10, (Table II) in ETP copper. Compared with the ETP copper welds, the OF copper welds displayed only a small quantity of gas porosity (see Figure 10). With the same welding parameters, all the OF copper welds, except weld 20, exhibited slightly greater penetration and upper bead width than the ETP copper welds (compare welds 16, 17, 19, 20 with welds 3, 4, 10 and 6, respectively, in Table III).

At the high welding speed of 25.4 mm/s (60 in/min), the OF copper weld (test 20) displayed a smooth metal overflow compared with the erratic metal overflow of the ETP copper weld (test 8), (see Figures 6 and 11). Moreover, the OF copper welds were relatively clean and indicated little evidence of copper oxide particles in the microstructure (see Figure 12) compared with the welds in ETP copper.

3.3 Ultrasonic Inspection of Copper Electron Beam Welds

3.3.1 C-Scan Maps

Three pairs of ETP copper and OF copper welds were selected for ultrasonic inspection. Each pair was made using the same combination of welding parameters. The C-scan computer image maps of these welds are shown in Figures 13, 14 and 15. A change in intensity on the maps indicates a different amplitude of the reflected signal/3/. A white area indicates a large signal amplitude, followed by dark grey and then light grey (vertical lines) in decreasing order of signal amplitude. The white areas are interpreted as weld discontinuities, such as lack of fusion and large cavities, and the dark areas as small cavities due to gas porosity/3/. The vertical, light-grey areas are interpreted as sound metal.

It is important to note that the normal-beam pulse-echo technique used did not give a complete evaluation of the weld samples. When the probe was placed near the sample edge, invisible or shadowed areas occurred (see Figure 2). This meant the quality of certain areas of the weld, which included part of the start and stop of the weld, as well as part of the upper bead and underbead, could not be inspected using this technique. In the following subsections, these C-scan maps are interpreted by comparing them with micrographs of cross sections prepared from the corresponding welds.

3.3.2 Welds 3 and 16

These welds were made at relatively low beam power (13.5 kW) and low welding speed (5.1 mm/s). Cross sections of welds 3 and 16 are shown in Figures 3(b) and 10(a), respectively. Both welds penetrated only partially through the workpieces.

The ETP copper weld in test 3 exhibited considerable gas porosity and a root cavity. The white areas of the corresponding C-scan map (see Figure 13(a)) appear to correlate with the root cavity and the unwelded interface, whereas the dark areas appear to show the presence of extensive gas porosity in the fusion zone.

The OF copper weld in test 16 exhibited a small quantity of gas porosity and a root cavity. In addition, because of the angular path of the electron beam, the underbead of the weld had missed the interface about midsection of the workpiece. The missed joint and the root cavity were not revealed on the C-scan map (Figure 13(b)). No dark areas were found on the map, suggesting that the lightly dispersed porosity was not

detected. The small scattered white areas on the map are likely related to the presence of scattered cavities in the fusion zone.

3.3.3 Welds 6 and 19

Welds 6 and 19 were made at relatively high beam power (20 kW) and welding speed (7.6 mm/s) compared with welds 3 and 16. The cross sections of these welds are shown in Figures 3(d) and 10(c). Both welds penetrated through the full thickness of the workpieces (ie, penetrations > 25 mm).

The ETP copper weld in test 6 contained a considerable amount of gas porosity and relatively large cavities in the fusion zone (see Figure 3(d)). The scattered dark areas and white areas on the corresponding C-scan map (see Figure 14(a)) appear to correlate to the gas porosity and cavities, respectively. The large white areas, which were at the weld initiation and termination sites, appear to show large unfused areas near these regions.

The OF copper weld in test 19 contained only a small quantity of scattered gas porosity in the fusion zone (see Figure 10(c)). The corresponding C-scan map (Figure 14(b)), however, did not appear to reveal the presence of this porosity. The small white areas on the map are probably related to isolated cavities in the fusion zone.

3.3.4 Welds 9 and 20

These welds were made at extremely high beam power (42 kW) and high welding speed (25.4 mm/s for weld 20 and 33.9 mm/s for weld 9). The cross sections of these welds are shown in Figures 6(a) and 10(d). Both welds penetrated through the entire thickness of the workpieces.

As shown in Figure 6(a), the ETP copper weld in test 9 contained a considerable concentration of cavities in the fusion zone, which appear as white and dark areas in the C-scan map (see Figure 15(a)). However, the large root cavity was not revealed on the C-scan map.

The OF copper weld in test 20 displayed a small quantity of gas porosity and a large cavity in the fusion zone (see Figure 10(d)), neither of which were revealed in the C-scan map (see Figure 15(b)).

4.0 DISCUSSION

4.1 Weld Penetration and Weld Profile

The proposed container joint design for the present application, shown in Figure 1/1/, contains an integral backing support and requires a weld penetration greater than 25 mm (preferably 30 to 35 mm). The present investigation has shown that square butt welds with depths of penetration greater than 25 mm can be made in 25-mm thick ETP and OF copper plate (ie, with a backing plate) using the EB welding process, without preheat.

It is generally known that, in EB welding, weld penetration increases with increasing beam power. The present study has shown that the beam power, and thus the weld penetration, can be increased by increasing either the voltage or the current. At higher power levels, the fusion zone of some of the EB welds also appeared to be more parallel-sided and displayed a wider underbead profile.

At a constant heat input of 26.6 kJ/cm (ie, welds 1 to 7), both the weld penetration and fusion zone area increased with increasing beam power and increasing weld speed. Previous studies/4/ have shown that greater fusion-zone area and penetration can be achieved at higher power levels for a constant heat input. In addition, at a given heat input, high welding speed promotes greater penetration since little time is available for lateral melting and a greater depth can thus be melted, leading to greater penetration/5/. For materials with a high thermal conductivity, such as copper, a relatively high welding speed is thus preferred, to promote penetration and to reduce excessive lateral melting. Welds 8 and 9, which were made at very high beam power and high welding speeds, displayed deep penetration (ie, > 25 mm) at relatively low heat input levels. In summary, the present investigation indicates that combinations of high beam power and high welding speed provide optimum penetration with minimum heat input in copper plate.

With the same welding parameters, slightly greater penetration was obtained in OF copper than in ETP copper. Since, OF copper has a slightly higher thermal conductivity than ETP copper/6/, greater penetration might be expected in the ETP copper. In previous studies/4/, greater penetration was observed in OF copper than in phosphorus deoxidized (DLP and DHP) copper, despite the fact that the former has the higher thermal conductivity. This was explained by the fact that the vapour pressure caused by impurities during welding affected the depth of penetration more than did slight variations in thermal conductivity (ie, OF copper is more pure than DLP and DHP

copper). Thus, the slightly lower depth of penetration displayed by ETP copper compared with OF copper for the same welding parameters could be explained by the higher impurity levels in the ETP copper, despite its lower thermal conductivity.

In the present study, copper EB welds were made at different focus positions below the surface, ie, 8.5 mm, 16.9 mm and 25.4 mm. The results appear to indicate that the focus position has no significant effect on depth of penetration. However, a focus position 8.5 mm below the surface appears to promote a more parallel-sided fusion zone in the EB welds.

4.2 Porosity, Cavities and Metal Overflow

4.2.1 Electrolytic Tough-Pitch Copper

Previous studies/4/ have shown that porosity in copper EB welds increases with increasing beam power and with decreasing welding speed. In the present investigation, a considerable amount of spherical gas porosity was found in the ETP copper EB welds, which were made at low welding speed, in the range of 3.4 to 8.5 mm/s (8 to 20 in/min), despite the fact that relatively low beam power was used (ie, 8.75 to 20.0 kW). At high welding speeds, 25.4 mm/s (60 in/min) and 33.9 mm/s (80 in/min), ETP copper welds 8 and 9 displayed only a small amount of gas porosity, although higher beam power (42 kW) was used. Apparently, high welding speed suppressed the evolution of dissolved gases, such as oxygen, and the formation of gas porosity in the fusion zone. Focus position, on the other hand, appeared to have no significant effect on the resultant porosity. Compared with all other parameters, welding speed appeared to have the greatest effect on porosity in copper.

At high welding speeds (ie, 25.4 mm/s and 33.9 mm/s), large cavities were detected in the mid-section and lower part of the fusion zones of welds 8 and 9. Previous EB welding studies/7/ have shown that, in some cases, the molten metal solidifies faster near the top and bottom of the weld than at the mid-section. When this occurs, the gas and metal vapour at mid-thickness can be trapped in the weld, forming cavities and porosity. In the present investigation, extremely high welding speeds seemed to promote this type of solidification. Such cavities were not found in welds made at relatively low welding speeds (ie, $\leq$ 8.5 mm/s). A previous study found that the formation of these cavities could be minimized by using the beam oscillation technique/7/, in which solidification starts at the bottom and ends at the top of the weld, without delayed solidification around the mid-section and lower part of the weld. In

this case, gas and metal vapour can escape and cavity formation does not occur. The EB welding machine used in the present investigation is not equipped with a beam oscillation facility. Therefore, lower welding speeds (ie < 25.4 mm/s, but > 8.5 mm/s) should be investigated in future work, to prevent the formation of cavities in the fusion zone.

Extremely high welding speeds promoted erratic metal overflow and blow holes on the surface of ETP copper welds 8 and 9. However, this was not observed in OF copper welds for comparable welding speeds. It appeared that the fused metal cooled at a much faster rate at high welding speeds, which, for ETP copper, led to violent gas-metal interaction as dissolved gases such as oxygen evolved from the surface of the weld.

Root cavities were found in some of the welds, particularly in those that did not penetrate the full thickness of the material. The root cavities occurred mostly in welds with a narrow fusion zone at the root of the weld, probably because the metal vapour generated at the centre of the molten column was unable to escape though the narrow slot at the bottom of the joint interface. Upon condensation and solidification, a cavity formed. In general, wide welds minimize the occurrence of root cavities since this provides a greater opportunity for metal flow into the cavity. In the proposed joint designs shown in Figure 1, any root cavity would be embedded either in the top lid or in the wall of the copper container, depending on joint design, which presumably would not significantly affect the integrity of the weldment.

4.2.2 Oxygen-Free Copper

The maximum allowable oxygen content in OF copper is ~0.001%/2/. The OF copper welds contained only a small quantity of gas porosity. Welding parameters, including the welding speed, appeared to have no significant effect on the quantity of porosity observed. Due to the low dissolved gas content, erratic metal overflow and blow holes on the weld surface were not observed. However, at a high welding speed of 25.4 mm/s (test 20), a cavity was detected at the bottom of the weld, extending the length of the weld, which was likely related to the solidification pattern of the weld at high welding speed.

4.3 Copper Oxide

In Phase One of this research program, melt runs were made on a 50-mm-thick ETP copper plate. Copper oxides were found as discrete particles in the grain interior and as a semi-continuous film at the grain boundaries, near the centres of several welds/1/. In the present study, all ETP copper welds

displayed a considerable amount of copper oxide as discrete particles in the grain interior, however, no grain boundary oxide films were detected in these welds. Variations in the welding parameters appeared to have no effect on the distribution and morphology of the copper oxide particles. For the OF copper welds, very little copper oxide was found in the form of discrete particles and no oxide films were detected. As discussed previously, small volume fractions of copper oxide, when dispersed uniformly throughout the structure, have little effect on the properties of a joint/1/, however, oxide films at the grain boundaries may cause weld embrittlement.

4.4 Missed Joint

In several welds, the narrow root spike missed the joint line as a result of misalignment between the electron beam and the butt weld joint. The alignment of the electron gun with the joint line was performed using low-power beam scanning. Although the beam was accurately focussed on the top of the joint line, the lower part of the interface was missed in several welds that had a relatively narrow underbead profile. It appears likely that the electron gun carriage rails were not parallel with the copper workpiece so that the electron beam struck the workpiece at a slight angle to the vertical, missing the lower part of the interface because of the angular path of the beam through the workpiece. Nevertheless, the results indicate that EB welds with a wide underbead can accommodate some slight misalignment between the electron beam and the weld joint and still produce complete fusion of the joint.

4.5 Ultrasonic Inspection

In this investigation, the copper EB welds were inspected using the normal-beam, fusion-line, pulse-echo technique. It was shown that potentially valuable information on weld quality near the upper bead and underbead was lost when the probe was placed near the edge of the welded sample. In the proposed joint design shown in Figure 1, however, the ultrasonic inspection probe can be positioned directly adjacent to the underbead, to give a full evaluation of the quality of the underbead, since there would be no "edge" effect. However, the fusion zone for some distance from the top of the weld would still not be detected because of the limited accessibility of the ultrasonic beam to this region. Based on the present observations, the quality of the upper bead might be assessed against the appearance of the metal overflow and the amount of blow holes on the surface of the weld. This aspect of the inspection of closure welds in copper requires further study.

It was also noted that areas of gas porosity in the fusion zone appeared as dark areas on the C-scan maps. The smallest pore that can be detected by ultrasonic inspection in copper welds is considered to be 1 to 2 mm in diameter, although this requires further verification. However, the porosity generally detected in the present study was less than 0.3 to 0.4 mm in diameter. For the OF copper welds, porosity was sparsely scattered through the fusion zone and was not detected by ultrasonic inspection. On the other hand, in the copper ETP copper welds in which significant porosity occurred, the reflected signals from individual pores appear to have interfered with each other and intensified. The resultant intensified signals from regions of porosity were therefore, revealed as dark areas on the C-scan maps. Thus, C-scan mapping appeared to qualitatively reveal the presence of porosity, but could not detect individual pores. Further studies should be carried out to determine the minimum size of pore that can be detected by ultrasonic inspection techniques. In addition, the intensified signals from areas of gas porosity should be quantitatively interpreted.

The present study showed that cavities ~1 to 3 mm in width or height were readily detectable using the ultrasonic inspection technique. These cavities were shown as white areas in the C-scan maps.

From the results of the present study, it was uncertain if a missed joint could be detected using the ultrasonic inspection technique. For example, ETP copper weld 3, the missed joint and the root cavity appeared as white areas on the C-scan map; however, the missed joint in OF copper weld 16 was not detected. More work is required to determine if a missed joint can be reliably detected and whether this is related to the ultrasonic inspectability of the materials, ie, OF and ETP copper.

4.6 Empirical Equation for Penetration in Copper Electron Beam Welds

The results have shown that the same penetration can be achieved by several combinations of welding parameters, each combination providing its own value of energy or heat input per unit length. In previous studies, Hashimoto and Matsuda/8/ developed mathematical relationships to predict weld penetration from the parameters used to make the weld. Their basic equation for penetration was

$$P = kA\, E^{\alpha}\, I^{\beta}\, \frac{1}{\psi\, S^{\delta}} \qquad (1)$$

where

P = penetration (mm); kA = material constant;
E = accelerating voltage (kV); I = beam current (mA);
S = welding speed (mm/s), ψ = beam spot size (mm);
α, β, δ = coefficients for E, I and S respectively.

The above equation was based on experimental results obtained on a 1.5 kW welding unit using an accelerating voltage between 30 and 50 kV. Johnson/4/, pointed out that the beam spot size changed with power level and that Hashimoto's work did not take this into account. The beam spot size determines the energy density, which is an important factor for controlling weld penetration in EB welding. However, at the present time there is no reliable and accurate method to measure the spot size, and thus the energy density, particularly when high power is used. At high-power levels, the "spot" actually comprises luminous vapours rather than molten material. In our present study, considerably higher power levels were used, ie, in the range 8.75 to 42 kW. An empirical equation was developed for weld penetration using the data obtained from this investigation:

$$P = K\, E^{a}\, I^{b}\, \frac{1}{S^{c}} \qquad (2)$$

where P,E,I, and S are as defined in Equation (1);

a, b and c are the coefficients for E, I and S;
K is a material constant.

In the current approach, the spot size (ψ) was incorporated into the material constant K. In the present study the beam spot size was not measured.

Linear regression analysis was performed using all the penetration data for the ETP and OF copper EB welds (Table II). As noted earlier the difference in weld penetration between ETP and OF copper welds made with the same welding parameters was quite small. Hence, in the present analysis, no distinction was made between the ETP and OF copper welds. By using all the penetration data, the material constant (K) and the coefficients, a, b and c, for voltage (E), current (I) and travel speed (S), were estimated (see Table IV) and the resulting equation for the weld penetration was found to be

$$P = 0.003\, \frac{E^{1.58}\, I^{0.64}}{S^{0.42}} \qquad (3)$$

The predicted weld penetration for each set of test parameters, calculated from Equation (3), is plotted against the actual weld penetration in Figure 16. For the welding parameters used, it appears that the weld penetration in copper electron beam welds can be quite reasonably estimated using Equation (3). The assumption that the change of spot size with beam power does not have a significant effect on weld penetration of thick copper appears to be valid within the range of power levels used in the present study.

5.0 FUTURE WORK: PHASE THREE

5.1 Phase 3A: Optimization of Welding Parameters

Single pass, square butt joints will be made in both OF and ETP 25-mm-thick copper plates (with backing plate), using various combinations of high power and high welding speeds to select the combinations of weld parameters that provide welds with minimum gas porosity, no fusion-zone cavities and a smooth metal overflow on the weld surface. The weld penetration should be at least 25 mm and preferably 30 to 35 mm.

For OF copper, the highest 'tolerable' welding speed that does not result in the formation of fusion-zone cavities will be determined. The most suitable high power/high welding speed combination will then be selected to give electron beam welds with the required penetration at the minimum heat input.

For ETP copper, because of its relatively high dissolved oxygen content, the allowable range of welding parameters, particularly the welding speed, is quite narrow. The welding speed should be considerably greater than 8.5 mm/s to reduce the gas porosity but lower than 25.4 mm/s to prevent the formation of fusion-zone cavities, or erratic metal overflow and blow holes on the weld surface. The welding parameters that produce the best weld quality will be identified.

In addition, the most suitable procedures for the initiation and termination of welding, ie the current slope-up and slope-down times, will be identified.

5.2 Phase 3B: Electron Beam Welding of Simulated Container Closure

Simulated container closure will be demonstrated by EB welding of small-scale copper pipe mockups (wall thickness = 25 mm), using the most suitable welding procedure identified in Phase 3A. Other factors, including seam tracking and ultrasonic inspection of the welds, will also be investigated in this phase of the work.

6.0 CONCLUSIONS

(1) Square butt, EB welds with penetration greater than 25 mm can be made in ETP and OF copper plates. High beam power/high welding speed combinations appear to provide optimum weld penetration at minimum heat input. An empirical equation has been developed to estimate the weld penetration for different combinations of weld parameters.

(2) The OF copper exhibits excellent weldability because of its extremely low dissolved oxygen content. Sound welds with deep penetration can be made using a wide range of welding parameters. The only apparent limitation is that the welding speed must be lower than 25 mm/s to prevent the formation of fusion-zone cavities.

(3) Due to the relatively high level of dissolved oxygen in ETP copper, sound welds can only be made using a narrow range of welding parameters. The welding speed has to be appreciably greater than 8.5 mm/s to reduce gas porosity, but must be lower than 25 mm/s to prevent the formation of fusion-zone cavities as well as blow holes and erratic metal overflow on the weld surface.

(4) Root cavities were found in most of the copper welds, which is typical for partially penetrated EB welds in thick material. In the proposed joint designs, however, any root cavities would be embedded either in the top lid or in the container wall, and should not significantly affect the integrity of the weld.

(5) In several welds the lower part of the butt joint was missed by the electron beam, although the beam had been accurately focussed on the joint line. It appeared that the electron beam struck the surface at a slight angle to the vertical because the electron gun carriage rails were not parallel with the copper workpiece.

(6) Nondestructive evaluation of the test welds by ultrasonic inspection indicated that relatively large cavities (width and length $\geq$ 0.8 mm) and densely populated small gas porosity (diameter $<$ 0.3 to 0.4 mm) can be detected using the fusion-line, pulse-echo technique. However, sparsely scattered gas porosity of the same size range cannot be detected. It is also questionable whether a missed joint defect can be detected, or whether the fusion zone near the edge or surface of the workpiece, can be adequately inspected using the above technique.

(7) The requirements for Phase Three of the copper electron beam welding program have been defined. They are to identify the optimum welding procedures for OF and ETP copper and to demonstrate final closure on small-scale copper pipe mockups.

ACKNOWLEDGEMENTS

The author wishes to thank F. Smith and J. Galloway for carrying out the metallographic examinations, and the technical personnel in the Nondestructive and Fracture Evaluation Section for performing the ultrasonic inspection studies. Appreciation is also extended to the Manufacturing Technology Centre at the National Research Council for their support in performing the welding trials. The author is also indebted to C.J. Schwarz for developing the empirical penetration equation and to M.J. Tinkler for his helpful comments in the preparation of this report.

Recommended:

B. Mukherjee
Supervising Engineer (Ag)
Metallurgical Research Dept

Submitted:

P.Y.Y. Maak
Engineer
Metallurgy Section

Approved:

O.A. Kupcis
Supervising Engineer
Metallurgical Research Dept

Reviewed by:

J.A. Chadha
Area Coordinator
AECL Technical Assistance Program

PYYM:ljh

REFERENCES

1. Maak, P.Y.Y., "Electron Beam Welding for Copper Spent Fuel Disposal Containers - Phase One", Ontario Hydro Research Division Report 82-378-K, December 1982.

2. 1982 Annual Book of ASTM Standards, Part 6, Copper and Copper Alloys, p. 333.

3. Tautt, G.A., Memo on Ultrasonic Inspection of Electron Beam Copper Welds, ND&FE, Ontario Hydro, November 4, 1982.

4. Johnson, L.D., "Some Observations on the Electron Beam Welding of Copper", Welding Journal, 1970, pp. 555-605.

5. Meheka, A.H., "Electron Beam Welding", McGraw-Hill Publishing Co Ltd for the Welding Institute, 1971, p. 98.

6. Metals Handbook, Vol 1, 8th Edition, American Society of Metals, 1961, p 55.

7. Tanaka, J., Kosuge, S. and Furawaka, H., "Electron Beam Welding for Heavy Section Steel Plates", International Conference on Welding Technology for Energy Applications, Gatlinburg, Tennessee, May 16-19, 1982.

8. Hashimoto, T and Matsuda, F, "An Equation for Calculating Optimum Welding Conditions in Electron Beam Welding", Trans National Research Institute for Metal (Japan), 7, pp. 21-26.

TABLE I

CHEMICAL SPECIFICATIONS FOR ELECTROLYTIC TOUGH PITCH COPPER (UNS No. 110) AND OXYGEN-FREE COPPER (UNS No. 101)

Element	OF Copper (UNS No. 101)	ETP Copper (UNS No. 110)
COPPER	99.99% min	99.9 % min
MERCURY	0.0001% max	0.001% max
PHOSPHOROUS	0.0005% max	0.005% max
ZINC	0.0001% max	0.001% max
CADMIUM	0.0001% max	0.0001% max
SULPHUR	0.0010% max	0.0010% max
LEAD	0.0010% max	0.0010% max
SELENIUM	0.0010% max	0.0010% max
TELLURIUM	0.0010% max	0.0010% max
BISMUTH	0.0010% max	0.0010% max
OXYGEN	0.0010% max	0.02-0.07% max
OTHER IMPURITIES	≈0.01%	≈0.01%

TABLE II

DETAILS OF WELDING TRIALS IN PHASE TWO

TEST WELD NO.	TYPE(1) OF COPPER	BEAM CURRENT (mA)	ACCELERATING VOLTAGE (kV)	WELDING SPEED mm/s (in/min)	FOCUS BELOW SURF mm (in)	POWER (kW)	HEAT INPUT(2) kJ/cm (kJ/in)
1	ETP	250	35	3.4 (8)	8.5 (1/3)	8.75	25.8 (65.6)
2	ETP	275	40	4.2 (10)	8.5 (1/3)	11.0	26.0 (66.0)
3	ETP	300	45	5.1 (12)	8.5 (1/3)	13.5	26.6 (67.5)
4	ETP	350	45	5.9 (14)	8.5 (1/3)	15.8	26.7 (66.7)
5	ETP	400	45	6.8 (16)	8.5 (1/3)	18.0	26.6 (67.5)
6	ETP	400	50	7.5 (18)	8.5 (1/3)	20.0	26.7 (66.7)
7	ETP	450	50	8.5 (20)	8.5(1/3)	22.5	26.6 (67.5)
8	ETP	700	60	25.4 (60)	8.5 (1/3)	42.0	16.5 (42.0)
9	ETP	700	60	33.9 (80)	8.5 (1/3)	42.0	12.4 (31.5)
10	ETP	350	45	5.9 (14)	16.9 (2/3)	15.8	26.7 (67.7)
11	ETP	350	45	5.9 (14)	25.4 (1)	15.8	26.7 (67.7)
12	ETP	325	45	5.9 (14)	8.5 (1/3)	13.5	24.7 (62.7)
13	ETP	375	45	5.9 (14)	8.5 (1/3)	16.9	28.5 (72.3)
14	ETP	350	40	5.9 (14)	8.5 (1/3)	14.0	23.6 (60.0)
15	ETP	350	50	5.9 (14)	8.5 (1/3)	17.5	29.5 (75.0)
16	OF	300	45	5.1 (12)	8.5 (1/3)	13.5	26.6 (67.5)
17	OF	350	45	5.9 (14)	8.5 (1/3)	15.8	26.7 (67.7)
18	OF	350	45	5.9 (14)	16.9 (2/3)	15.8	26.7 (67.7)
19	OF	400	50	7.5 (18)	8.5 (1/3)	20.0	26.7 (66.7)
20	OF	700	60	25.4 (60)	8.5 (1/3)	42.0	16.5 (42.0)

(1) ETP and OF stand for electrolytic tough-pitch copper and oxygen-free copper respectively.

(2) Heat Input is calculated as $\frac{\text{accelerating voltage (V) x beam current (A)}}{\text{welding speed (cm/s or in/s)}}$

TABLE III

WELD PENETRATION AND WELD WIDTH

TEST (1) NUMBER (TYPE OF COPPER)	PENETRATION (P) mm	WELD WIDTH		
		W1 mm	W2 mm	W3 mm
1 (ETP)	-	-	-	-
2 (ETP)	16.6	3.0	0.7	-
3 (ETP)	20.3	3.9	0.8	-
4 (ETP)	23.0	3.4	1.4	0.5
6 (ETP)	29.7	4.3	1.6	0.6
7 (ETP)	30.3	3.8	1.6	1.0
8 (ETP)	32.3	2.9	2.0	2.0
9 (ETP)	27.7	2.9	2.0	1.0
9* (ETP)	26.3	2.6	1.9	1.0
10 (ETP)	23.0	4.8	1.1	-
11 (ETP)	23.4	4.9	0.9	-
12 (ETP)	21.1	5.4	0.9	-
13 (ETP)	29.4	4.9	1.4	0.4
14 (ETP)	18.9	4.3	0.7	0.3
15 (ETP)	25.0	4.5	1.5	0.4
16 (OF)	22.6	4.3	0.9	-
16* (OF)	20.9	4.5	1.1	-
17 (OF)	26.6	5.0	1.2	0.4
19 (OF)	29.1	4.3	1.3	0.8
19* (OF)	30.6	4.6	1.4	0.9
20 (OF)	29.4	3.4	2.1	1.7
20* (OF)	28.6	3.6	2.1	1.7

(1) All the welded samples were sectioned at a location ~25 mm from the weld initiation except for those with a "*", which were sectioned at ~50 mm from the weld initiation.

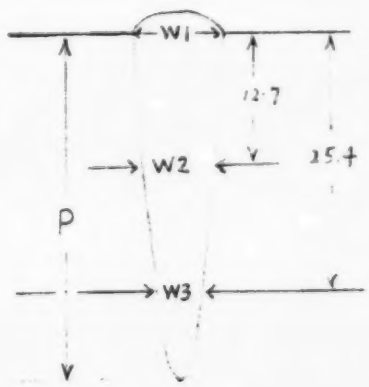

TABLE IV

PENETRATION EQUATION FOR ELECTRON BEAM WELDING OF THICK COPPER

Model Equation $P = K \frac{E^a I^b}{S^c}$

or $\ln P = \ln K + a \ln E + b \ln I - c \ln S$

From Linear Regression

	ln K	K	a	b	c
Estimates	-5.84	0.003	1.58	0.64	0.42
Standard Error	1.38	-	0.58	0.19	0.06

where P = penetration, mm
E = accelerating voltage, kV
I = beam current, mA
K = material constant
S = welding speed, mm/s
a,b,c = coefficients for E, I and S respectively

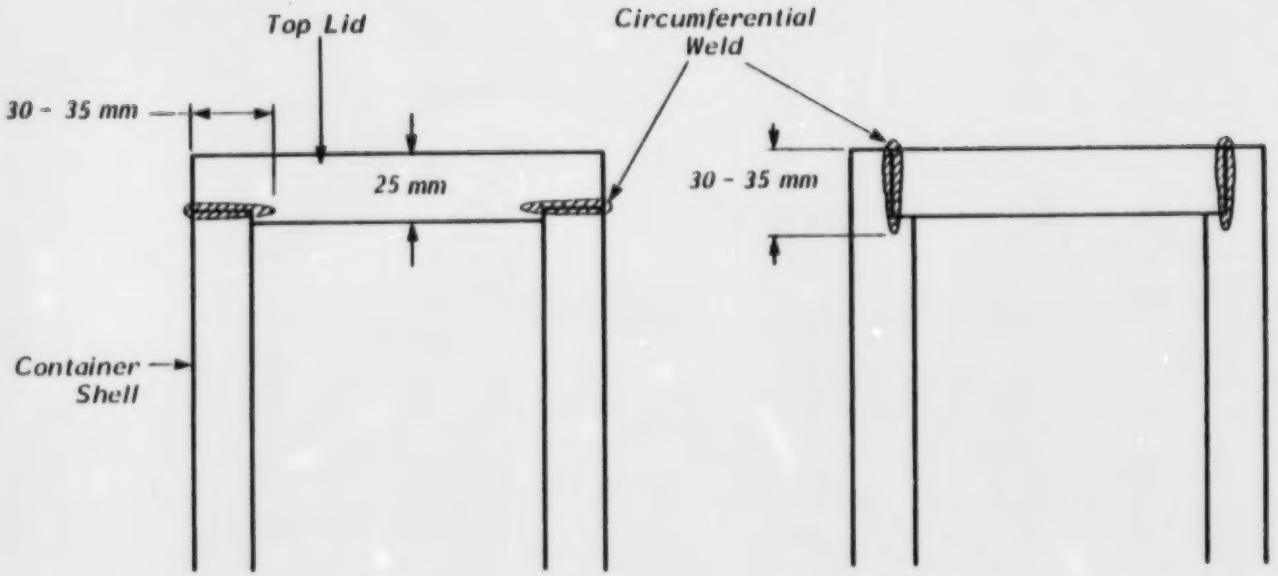

FIGURE 1

SCHEMATIC DIAGRAM SHOWING THE FINAL CLOSURE JOINT DESIGN WITH INTEGRAL BACKING SUPPORT FOR A COPPER CONTAINER FOR NUCLEAR FUEL-WASTE DISPOSAL

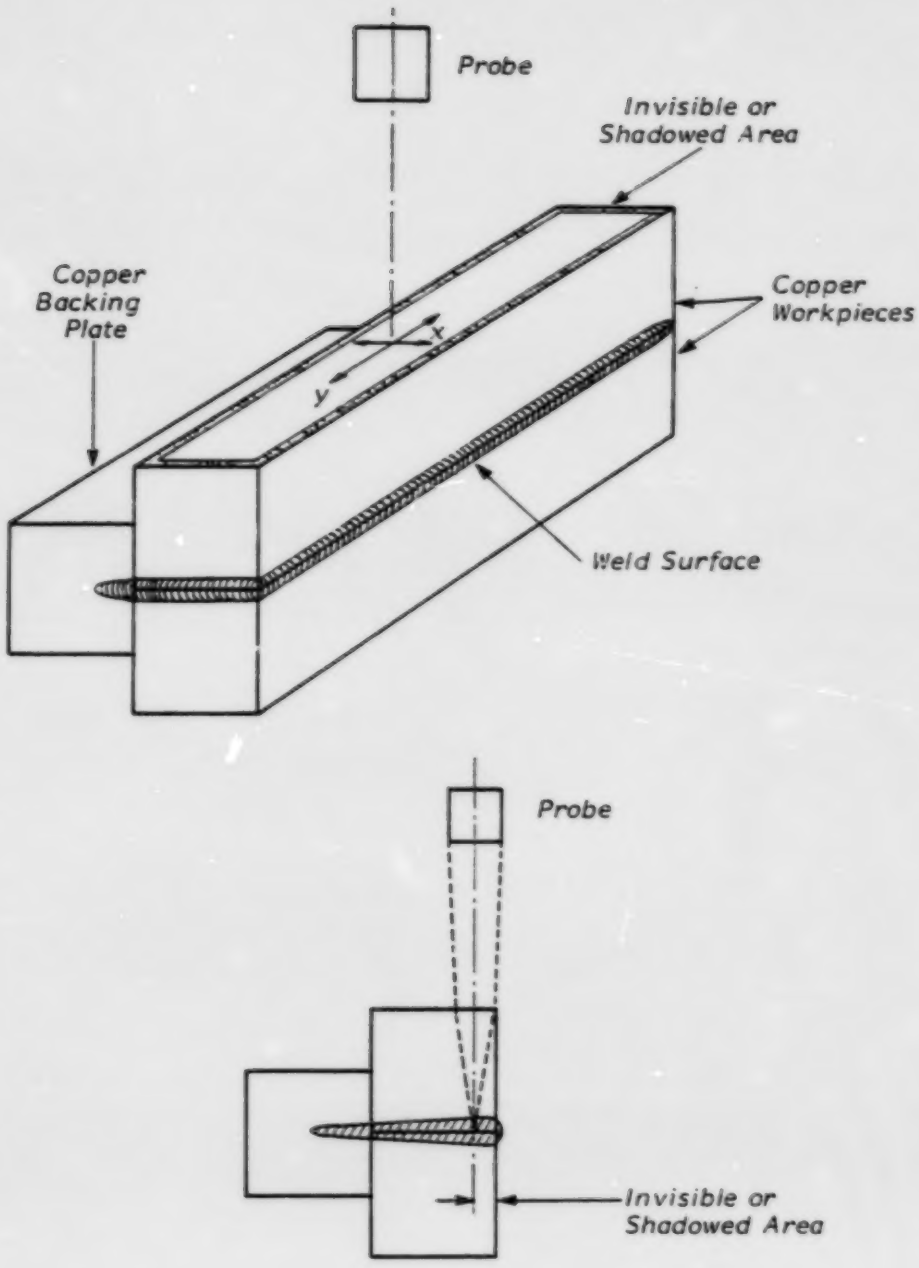

FIGURE 2

SCHEMATIC EXAMPLES SHOWING THE SET-UP FOR ULTRASONIC INSPECTION OF COPPER ELECTRON BEAM WELDED SAMPLES

163073 RD

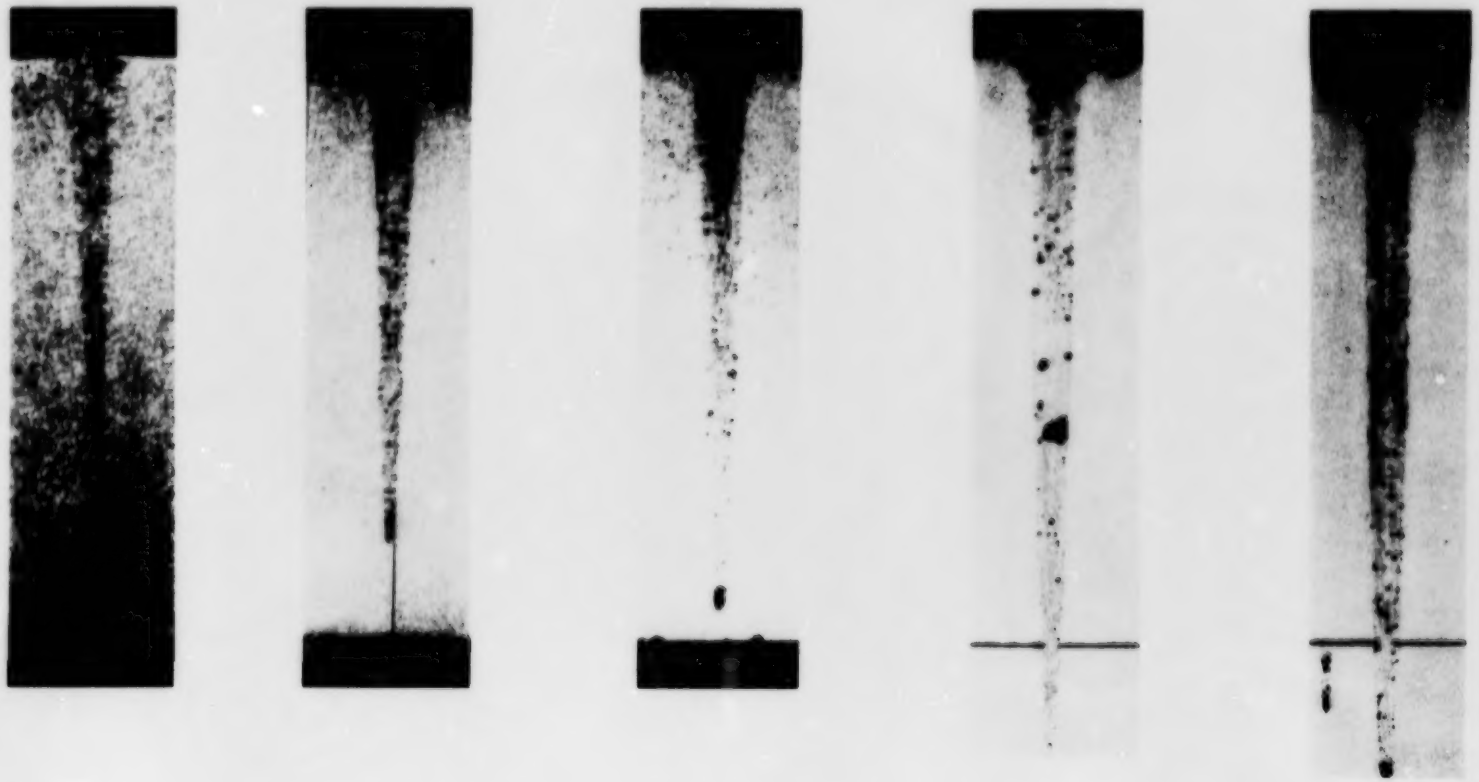

(a) Test number 2 (b) Test number 3 (c) Test number 4 (d) Test number 6 (e) Test number 7

84-57

FIGURE 3 - CROSS SECTIONS OF ELECTROLYTIC TOUGH-PITCH COPPER WELDS, MAG 3.5 X

FIGURE 4 - TYPICAL MICROSTRUCTURE OF ELECTROLYTIC TOUGH PITCH COPPER ELECTRON BEAM WELDS, MAG 600 X

a) Test number 1

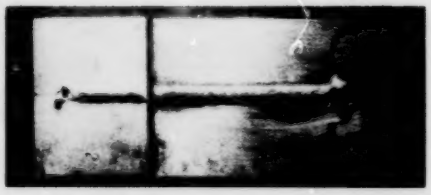

b) Test number 2

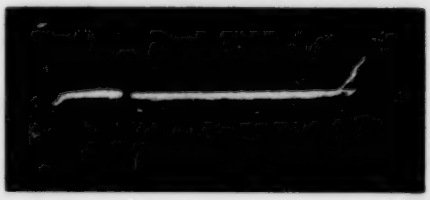

c) Test number 3

d) Test number 4

e) Test number 5

f) Test number 6

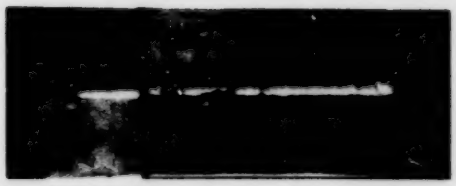

g) Test number 7

FIGURE 5 - SURFACE APPEARANCE OF ELECTROLYTIC TOUGH PITCH COPPER WELDS IN TESTS 1 TO 7

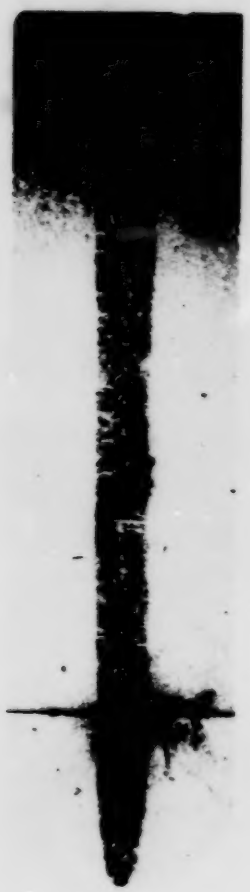

Test number 8

Test number 9

(a) Cross sections (Mag 3.5 X)

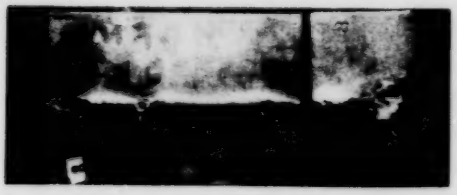

Test number 8

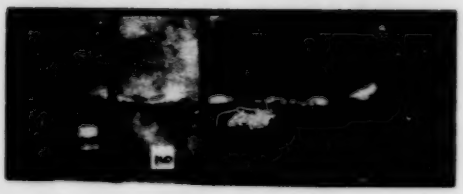

Test number 9

(b) Surface appearance (Mag 0.5 X)

FIGURE 6 - CROSS SECTIONS AND SURFACE APPEARANCE OF ELECTROLYTIC TOUGH-PITCH COPPER WELDS IN TESTS 8 AND 9

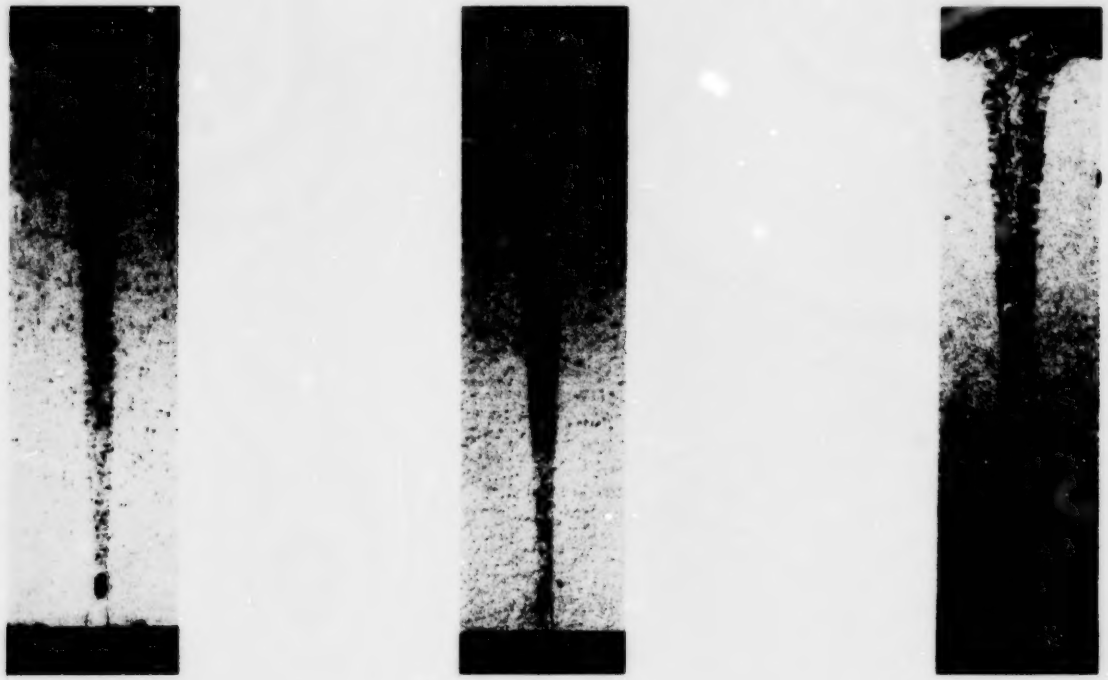

(a) Test number 4 (8.5 mm below surface)

(b) Test number 10 (16.9 mm below surface)

(c) Test number 11 (25.4 mm below surface)

FIGURE 7 - CROSS SECTIONS OF ELECTROLYTIC TOUGH PITCH COPPER WELDS MADE WITH ELECTRON BEAM FOCUSSED AT VARIOUS POSITIONS BELOW THE SURFACE , MAG 3.5 X

(a) Test number 12 (325 mA)

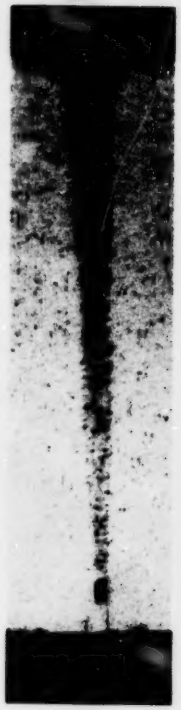

(b) Test number 4 (350 mA)

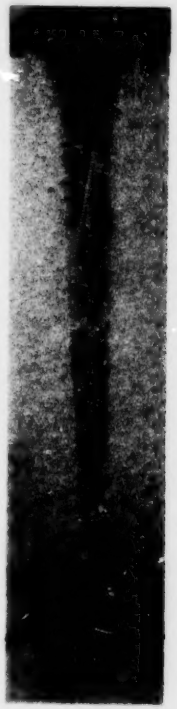

(c) Test number 13 (375 mA)

FIGURE 8 - CROSS SECTIONS OF ELECTROLYTIC TOUGH-PITCH COPPER WELDS MADE AT INCREASING WELDING CURRENT, MAG 3.5 X

(a) Test number 14 (40 kV)

(b) Test number 4 (45 kV)

(c) Test number 15 (50 kV)

FIGURE 9 - CROSS SECTIONS OF ELECTROLYTIC TOUGH-PITCH COPPER WELDS MADE AT INCREASING VOLTAGE, MAG 3.5 X

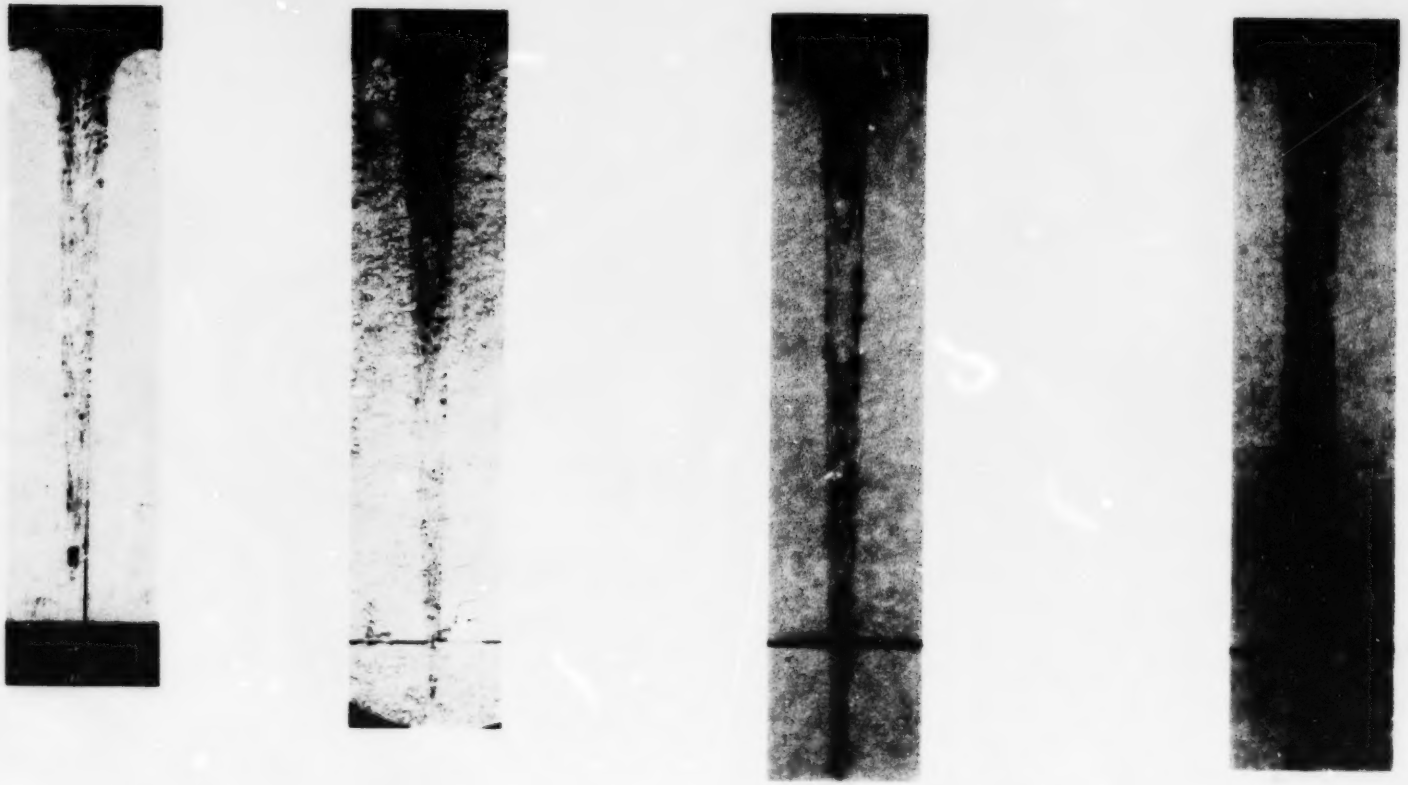

(a) Test number 16 (b) Test number 17 (c) Test number 19 (d) Test number 20

FIGURE 10 - CROSS SECTIONS OF OXYGEN-FREE COPPER WELDS IN TESTS 16, 17, 19 AND 20, (MAG 3.5 X)

(a) Test number 16

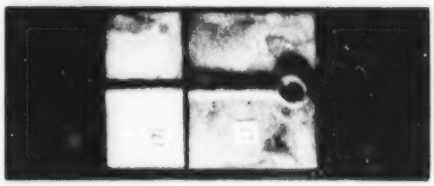

(b) Test number 17

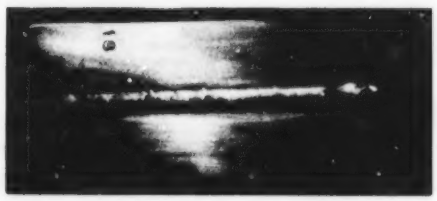

(c) Test number 18

(d) Test number 19

(e) Test number 20

FIGURE 11 - SURFACE APPEARANCE OF OXYGEN-FREE COPPER WELDS, MAG 0.5 X

FIGURE 12 - TYPICAL MICROSTRUCTURE OF OXYGEN FREE COPPER ELECTRON BEAM WELDS, MAG 600 X

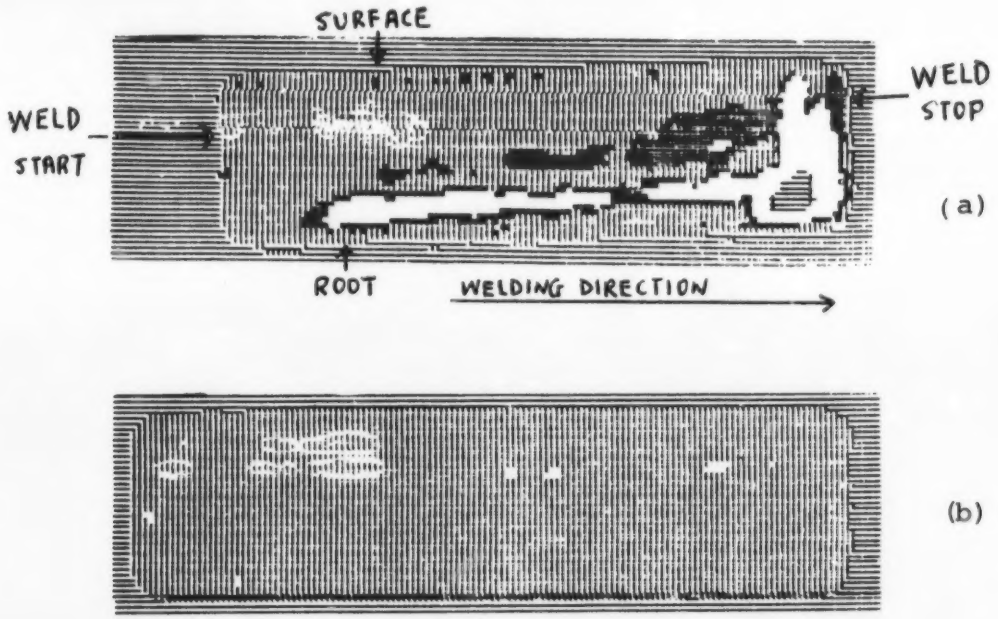

(a) Test number 3

(b) Test number 16

FIGURE 13 - C-SCAN MAPS FOR WELDS IN TESTS 3 AND 16

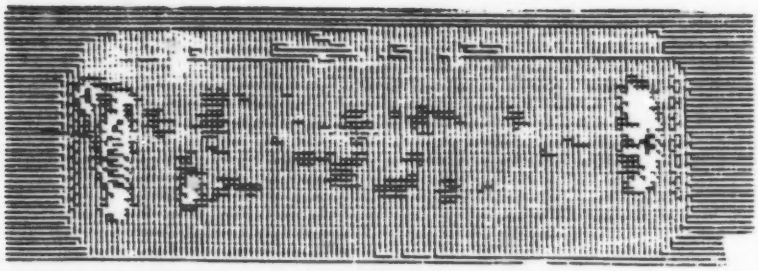

(a) Test number 6

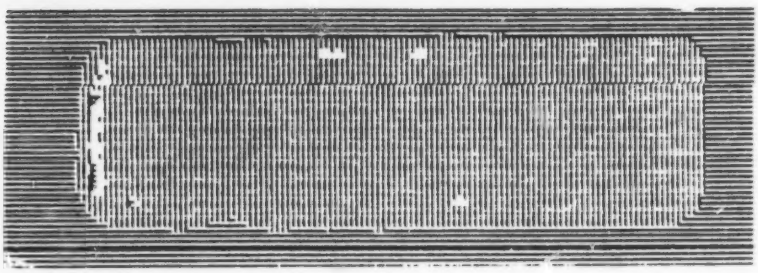

(b) Test number 19

FIGURE 14 - C-SCAN MAPS FOR WELDS IN TESTS 6 AND 19

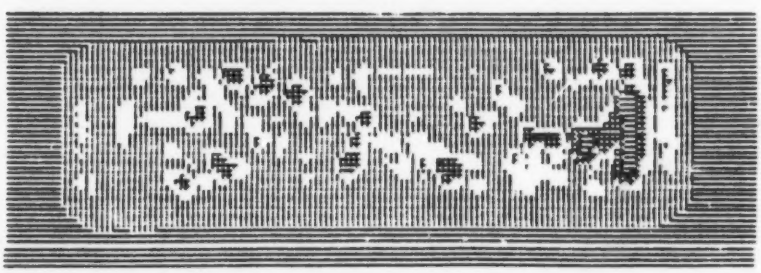

(a) Test number 9

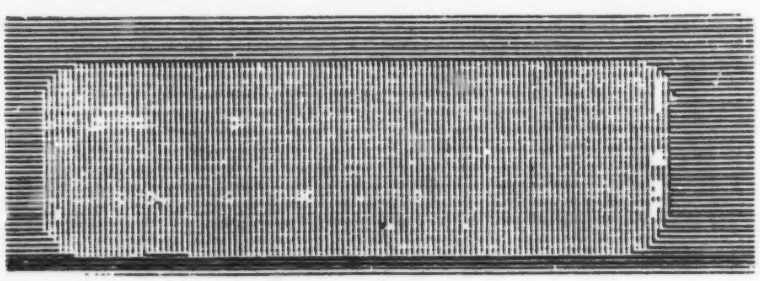

(b) Test number 20

FIGURE 15 - C-SCAN MAPS FOR WELDS IN TESTS 9 AND 20

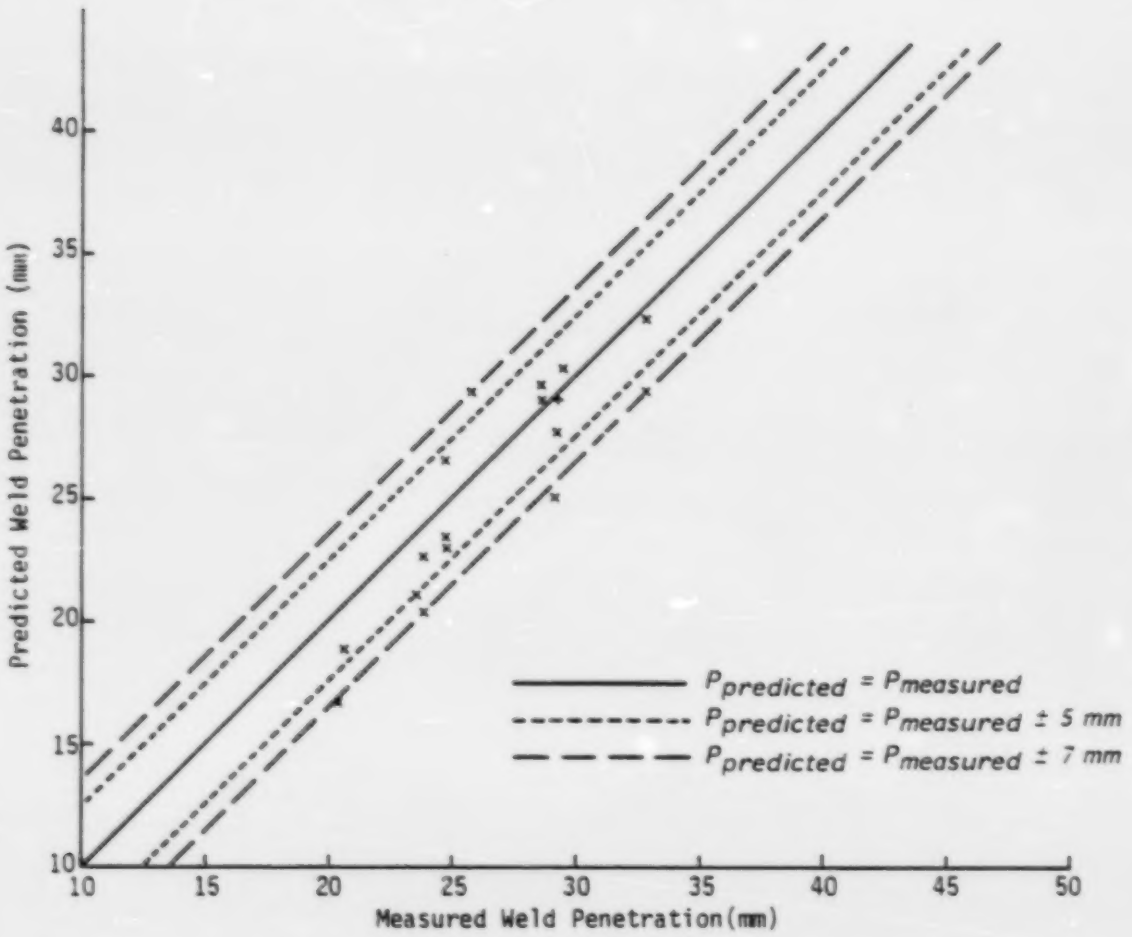

FIGURE 16

PREDICTED WELD PENETRATION VERSUS MEASURED WELD PENETRATION

163074 RD